Innovative Food Science and Emerging Technologies 66 (2020) 102528

Contents lists available at ScienceDirect

Innovative Food Science and Emerging Technologies

journal homepage: www.elsevier.com/locate/ifset

Water release kinetics from soy protein gels and meat analogues as studied with confined compression

Steven H.V. Cornet [a,b,*], Dylan Edwards [b], Atze Jan van der Goot [b], Ruud G.M. van der Sman [a,b]

[a] Food and Biobased Research, Wageningen University & Research, the Netherlands
[b] Food Process Engineering, Agrotechnology and Food Sciences Group, Wageningen University & Research, the Netherlands

ARTICLE INFO

Keywords:
Meat analogue
Confined compression
Juiciness
Flory-Rehner theory
Water release kinetics
Plant protein

ABSTRACT

In this paper, we report on the use of confined compression to study the water release properties from food gels and model meat analogues. Confined compression is a novel method in food science that provides information on the dynamics of water release under mechanical load. Confined compression measurements are compared with numerical simulations based on Flory-Rehner theory. Simulation results for soy protein gels are in reasonable agreement with experiments, while they underestimate the water release from model meat analogues. Time-domain nuclear magnetic resonance (TD-NMR) revealed the presence of internal water-filled cavities in the meat analogues. These cavities could provide a path of low resistance for the water to travel through. However, they are not captured by our current model, which explains the higher fluxes observed experimentally. Our results indicate a relation between the water release properties of meat analogues and pore structure. Control of the pore structure might, therefore, provide new opportunities to improve meat analogue juiciness.

1. Introduction

Reducing the consumption of meat products and transitioning towards a more plant-based diet could be beneficial to the environment (Aiking, 2011; Smetana, Mathys, Knoch, and Heinz, 2015). To ease this transition, meat analogue products that accurately mimic the sensory characteristics of real meat should be developed (Hoek, 2010). Some of the most important characteristics of meat are its flavour, fibrous texture, and juicy mouthfeel. The fibrous texture can already be mimicked with reasonable accuracy by processing mixtures of plant proteins in a Shear Cell (Dekkers, Nikiforidis, & van der Goot, 2016; Grabowska et al., 2016; Grabowska, Tekidou, Boom, & van der Goot, 2014; Schreuders et al., 2019). However, the number of studies dedicated to understanding and improving the juiciness of meat analogue products is limited (Cornet, Snel, Lesschen, van der Goot, & van der Sman, 2021; Cornet, van der Goot, & van der Sman, 2020).

The juiciness of real meat is related to the water holding capacity and the juice released during mastication (Warner, 2017; Winger & Hagyard, 1994). In meat, juiciness can be considered as a multistage or time-dependent sensation and can be divided into initial and sustained juiciness (Aaslyng, Bejerholm, Ertbjerg, Bertram, & Andersen, 2003; Bertram, Aaslyng, & Andersen, 2005; Warner, 2017). Bertram et al. (2005) showed that the spatial distribution and relative mobility of water in pork correlate with the perceived juiciness (Bertram et al., 2005). During (over-) cooking of meat, the water distribution changes due to denaturation of muscle proteins and contraction of the muscle fibre (van der Sman, 2007). Water is expelled from the myofibrils into the extracellular space before moving out of the meat entirely (Bertram et al., 2005; Bertram, Andersen, & Karlsson, 2001). The extracellular water has higher mobility and might, therefore, be more easily expelled than the water still bound to the myofibrillar proteins. The initial juiciness could, therefore, be related to water loosely held inside internal cavities, which is easily expelled during the first bite. The sustained juiciness could relate to the release of more tightly held water, which is expelled during continued mastication. The sustained juiciness is thought to be associated with the water holding capacity (WHC) and moisture content (Van Oeckel, Warnants, & Boucqué, 1999, Warner, 2017, Lucherk et al., 2017, Pearson and Dutson, 1994, Chapter 4–5). Additional factors such as fat content, flavour compounds, the presence of salts, and salivation by the consumer will probably also play a role in the sensory perception of juiciness (Warner, 2017).

An accurate meat analogue should also encompass these two stages of juiciness. Meat analogues can contain considerable volumes of air (Dekkers, Hamoen, Boom, & van der Goot, 2018; Tian, Wang, van der

* Corresponding author at: Food and Biobased Research, Wageningen University & Research, the Netherlands.
E-mail address: steven.cornet@wur.nl (S.H.V. Cornet).

https://doi.org/10.1016/j.ifset.2020.102528
Received 21 August 2020; Received in revised form 1 October 2020; Accepted 2 October 2020
Available online 17 October 2020

Goot, & Bouwman, 2018; Wang, Tian, van der Goot, & Boom, 2018). These cavities could be filled with fluid through impregnation. Water-filled cavities can affect the local resistance to flow (Tokita & Tanaka, 1991), and will alter the rate of water release from meat analogues. Cavities might also collapse, leading to further expulsion of water. Hence, the cavities could contribute to the initial juiciness. This study focuses on understanding the water release properties of porous model meat analogues and non-porous soy protein gels by studying the water release rate as a function of applied pressure over time.

We have designed a confined compression cell to measure the rate of water release from (food) hydrogels (Fig. 1). During confined compression a sample is deformed inside a water-permeable confined space using a texture analyser. The change in sample height is recorded and is a direct measure for the sample volume. When it is assumed that only water is expelled, the composition and water release rate can be determined in time. The ability to accurately track the sample volume during an experiment is the main advantage of confined compression over conventional unconfined compression. Confined compression is used in other fields to study the mechanical and hydration properties of soft materials such as collagen gels (Knapp et al., 1997), cartilage (Roos, Petterson, & Huyghe, 2013; Soltz & Ateshian, 1998), and agarose gels (Liu, Subhash, & Moore, 2011). To our knowledge, we are the first to report on the use of confined compression to study the hydration properties of food gels. Hence, an additional purpose of this paper is to showcase the capabilities of confined compression.

Furthermore, alongside the experimental work, we have developed a model to simulate the water release from a cross-linked polymer gel. The model is based on Flory–Rehner theory of polymer gel swelling (Flory & Rehner, 1943), and Darcy flow. The gel's local permeability is calculated based on the work by Tokita and Tanaka (1991). Using this combination of experiments and simulations we aim to improve our physical understanding of the relation between meat analogue structure and water release kinetics.

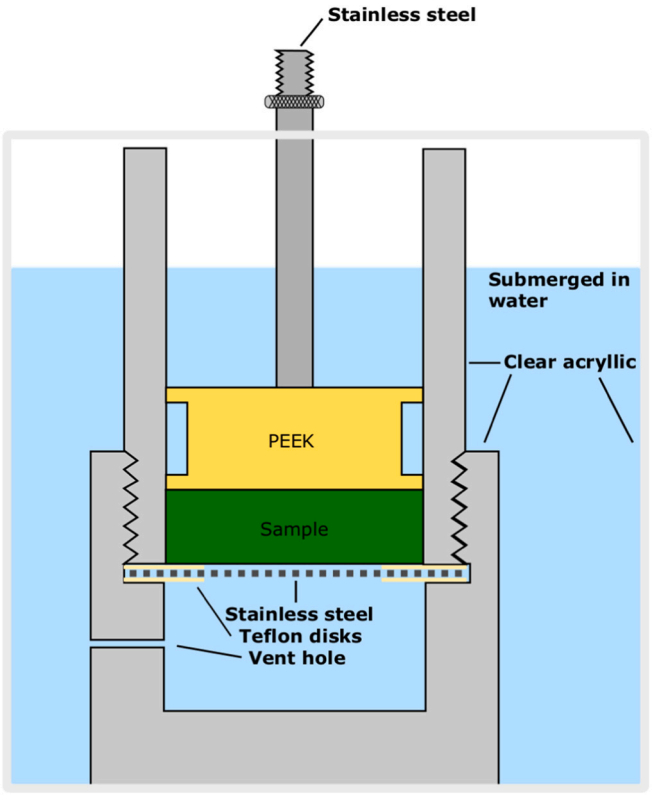

Fig. 1. Cross-sectional representation of the confined compression cell. Materials used are indicated in the figure. The steel shaft connects to an Instron texture analyser. The setup was submerged in water during experiments. Image is not to scale; relevant dimensions are described in the text.

2. Materials and methods

Before taking samples for the confined compression tests, the gels and model meat analogues were equilibrated with pure water. This puts them in a well-defined thermodynamic state. From the swollen materials, cylindrical samples were taken and transferred to the compression cell. The sample was compressed by a piston according to the load profile in Fig. 5 and the water release rates were determined. The evolution of the pore structure of the model meat analogues after compression was studied using time-domain nuclear magnetic resonance (TD-NMR). The water mobility distribution from TD-NMR provides insight into the mobility and the relative size of the different water populations, such as water present in the gel matrix or cavities. Model simulations of confined compression were run to better understand the water release from gels without pores.

2.1. Materials

Soy protein isolate (SPI; Supro 500E, Solae, St Louis MO, USA) and vital wheat gluten (gluten; Roquette, Lestrem, France) were obtained from commercial sources and were used as received. SPI and gluten had a protein content of 81.7±1.1 and 77.9±0.1 (Nx5.7) on a dry matter basis respectively. Sodium chloride (*NaCl*) and all other reagents used were of analytical grade and were obtained from Sigma-Aldrich (Steinheim, Germany). Milli-Q water was used for all experiments.

2.2. Methods

2.2.1. Production of soy protein gels

Soy protein isolate (SPI) gels were prepared according to Cornet et al. (2020). SPI powder was weighed and added to water to achieve the desired final dry matter content (DMC) (25, 30, 35 wt%). The protein dispersion was vigorously mixed by hand until a dough was obtained. The doughs were placed in vacuum bags and air was removed by applying a vacuum of 50 mbar for 45 s. The vacuumed doughs were stored overnight at 4°C to allow for full hydration. The moisture content of all hydrated doughs was measured after preparation (Section 2.2.4). Hydrated doughs were transferred to stainless steel gelation vessels (12.5 mm inner diameter; 5 mm inner height) and sealed hermetically. The sealed vessels were submerged in a Julabo water bath, pre-heated at 95 °C and shaken at a frequency of 100 rpm. After 30 min, the vessels were transferred to a water bath of approximately 15°C for 15 min to cool. Vessels were then opened and the gels were gently removed. After trimming the edges the final gel was obtained. The gels were allowed to swell as explained in Section 2.2.3.

2.2.2. Production of model meat analogues

Fibrous model meat analogues were prepared from SPI, gluten, *NaCl*, and water using a Couette-type shearing device similar to the one described by Krintiras, Diaz, van Der Goot, Stankiewicz, and Stefanidis (2016). An SPI:gluten:*NaCl*:water ratio of 15:15:1:69 was used, resulting in a DMC of 31 wt%. Samples had a height of 25 mm and were prepared as follows. *NaCl* was dissolved in water and the SPI powder was added and mixed using a *Z*-blade mixer (Winkworth Machinery Ltd., Basingstoke, UK). After a hydration period of 30 min gluten was added, followed by further mixing. The obtained mixture was transferred to the Couette shearing device. The Couette device was heated, and an average shear rate of 14.1 s^{-1} was applied for 35 min, during which the sample reached a temperature of 135°C. After shearing, the system was cooled down to 50°C after which the device was opened. The sample removed immediately and stored in a hermetically sealed bag to prevent moisture loss. After the model meat analogues reached room temperature (22 °C) they were stored at −18 °C until use to prevent spoilage.

2.2.3. Swelling pre-treatment

Gels and model meat analogues were swollen to equilibrium in an excess of Milli-Q water at 4°C before all confined compression experiments. A sample: water ratio of 1: 100 (wt: wt) was used for the SPI gels. Gels were swollen for at least 24 h during which the water was exchanged three times to wash away most ions present. Due to the larger size of the model meat analogues a sample: water ratio of 1: 20 was used, and the swelling time was extended to at least 72 h. The composition after swelling was determined by measuring the dry matter content (Section 2.2.4).

2.2.4. Dry matter content and maximum level of swelling determination

Dry matter content (DMC) was determined by drying at 105 °C for at least 24 h. The maximum level of swelling was determined based on the DMC in the swollen state. In our model we will use the polymer volume fraction in the fully swollen state φ_0 as a measure for swelling:

$$\varphi_0 = \frac{y_p/\rho_p}{(y_p/\rho_p) + (1-y_p)/\rho_w} \quad (1)$$

y_p and $(1 - y_p)$ are the dry and wet weight fractions as determined during oven drying. ρ_p and ρ_w are the density of polymer and water, respectively.

2.2.5. Confined compression

Description of the setup. Water release kinetics were measured using an in-house built confined compression cell (Fig. 1; Wageningen Technical Development Studio). The setup consists of an acrylic cylinder with an inner diameter of 40 mm that screws onto an acrylic bottom compartment. The bottom compartment has a vent hole to prevent pressure build-up. A stainless steel perforated plate rests in between the bottom compartment and the cylinder. The plate is covered with a fine steel mesh to provide both mechanical support and minimal flow resistance. The piston is made of poly-ether ether ketone (PEEK) and attached to a stainless steel shaft. The piston has an outer diameter approximately 20 μm smaller than the inner diameter of the cylinder to ensure a good fit. The piston shaft was attached to an Instron 5564 system outfitted with a 2 kN load cell, which was used to apply a range of loads. The confined compression cell was submerged in water during experiments to prevent evaporative moisture loss. A thin layer of water between the piston and cylinder walls was assumed to provide frictionless motion. Submersion in water gives a unique definition of the boundary condition, where the chemical potential of water μ_w equals zero.

The design of the confined compression setup bears a resemblance to earlier designs reported in literature (Knapp et al., 1997; Liu et al., 2011; Roos et al., 2013; Soltz & Ateshian, 1998). Liu et al. (2011) used a porous confinement cell and piston and thus allowed for water to leave the sample from all sides, while in the present design water could only leave the sample from the bottom of the sample. Knapp et al. (1997), Roos et al. (2013) and Soltz and Ateshian (1998) instead used a porous piston combined with impermeable sides and base. Roos et al. (2013) used both torsional and axial actuators to apply both compressive and rotational strains. All mentioned studies submerged the compression cell in water during the measurements. Furthermore, Roos et al. (2013) varied the ionic strength of the bath to study its effect on the shear modulus, which led to corrosion of their setup. All mentioned studies either did not discuss friction between the piston or sample and the confinement cell (Knapp et al., 1997; Liu et al., 2011; Soltz & Ateshian, 1998) or, like the present study, assumed frictionless motion due to a lubricating film of water (Roos et al., 2013).

Experimental procedure. Swollen samples were trimmed to a diameter of 40 mm using a cylindrical knife. Samples were submerged in water for at least 1 h after trimming to minimize its effect on sample water retention. The confined compression cell was submerged in water while making sure no air bubbles were entrapped inside the cell. The sample was then placed on the stainless steel plate inside the cylinder. The piston was lowered without touching the sample as observed through the transparent cylinder. The piston was attached to the load cell before starting the experiment.

To ensure the sample was properly seated, the piston was first lowered at a rate of 5 mm min^{-1} until the force exceeded 2 N. Then, a sequence of loads was applied with a deformation rate of 5 N s^{-1}. A lower rate of 2.5 N s^{-1} was used for the model meat analogues to reduce excessive crosshead movement. The duration of each load step was 300 s (5, 10, 15, 20, 25, 30, 35, 50 N; Fig. S1, right axis). The height at 3 N was taken as the initial height of the sample. Recorded parameters were time, force, and height.

Load-controlled experiments require a balance between the gain and rate of load application to prevent oscillations and (large) overshoots in the applied load. After preliminary experiments on swollen SPI gels, a gain of 0.02 mm N^{-1} was selected. This resulted in a limited overshoot with a duration of up to 1 s and a near-instantaneous load application (Fig. 2). The effect of the load overshoot on the measurements will be discussed with the results. Preliminary experiments with an empty cell confirmed that the confined compression cell does not significantly deform during the experiment.

Data analysis. The volumetric flux of water release, j, was deduced from the incremental volume change over time step dt:

$$-j(t) = \frac{dH}{dt} \quad (2)$$

The polymer volume fraction at time t $\varphi(t)$ was deduced from the initial polymer volume fraction φ_0, initial height H_0, and actual height $H(t)$ assuming incompressibility and the absence of air:

$$\varphi(t) = \frac{H_0}{H(t)}\varphi_0 \quad (3)$$

The swollen soy protein gels were analysed in triplicate, which were averaged and used to calculate standard errors. For the swollen model meat analogue, two duplicates with three replicates each were recorded. Since there was some variation in the initial and final DMC of the model meat analogues, individual data sets were analysed by calculating the flux over periods of 5 s.

2.2.6. Time-domain nuclear magnetic resonance (TD-NMR)

Time-domain NMR (TD-NMR) experiments were performed on a Maran Ultra NMR spectrometer with a field strength of 0.72 T (30.7 MHz ^{1}H resonance frequency) and controlled with the RINMR software

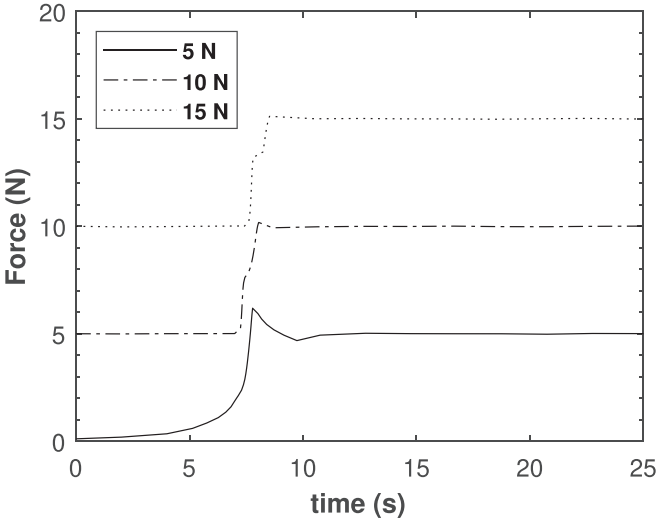

Fig. 2. Raw force data as function time for a swollen 25 wt% SPI gel showing the increase in measured force. The 10 N and 15 N lines are offset by 300 s.

package (Resonance Instruments Ltd., Witney, UK). A protocol similar to Schreuders, Bodnár, Erni, Boom, and van der Goot (2020) was used, which consisted of a Carr-Purcell-Meiboom-Gill (CPMG) echo train with 5 data points per echo and a total of 12,288 echos. A sampling time of 10 μs resulted in a spectral width of 100 kHz. The time between echos was 500 μs. 16 transients were recorded with phase cycling and a relaxation delay of 10 s, which were averaged to a single data point. All TD-NMR experiments were performed in triplicate and analysed using the IDL software package (ITT Visual Information Solutions, Boulder, CO, USA). The CONTIN fit routine was used to determine the water mobility distributions (Provencher, 1984). Intensities were normalized to the highest intensity within a single data set. Peak areas were determined using the trapezoidal method in Matlab.

2.2.7. Compression by centrifugation

Studying the effect of compression on the internal pore structure required an alternative method of compression as sampling during a confined compression experiment is not possible. Therefore, a centrifuge was used as an alternate means of applying an external pressure, Π_{ext}. The combination of centrifugation and TD-NMR has been used previously by (Bertram, Dønstrup, Karlsson, & Andersen, 2002). Samples were trimmed to a diameter of 5 mm using a biopsy punch and placed inside the upper compartment of centrifugal filtration tubes. The tubes have two compartments separated by a filter (pore size 0.2 μm; Pall Centrifugal Devices, Medemblik, The Netherlands). During centrifugation in an Eppendorf bench-top centrifuge, the expelled fluid was collected in the bottom compartment. A swinging bucket rotor was used to ensure that the axis of deformation was parallel to the axis of load application. Samples were centrifuged for 1 h at different centrifuge speeds, which was long enough to reach equilibrium. Samples were transferred to NMR tubes immediately after a centrifugation step was completed and their water mobility distribution was recorded (Section 2.2.6). Furthermore, the amount of expelled water was determined by weighing. A range of external pressures was applied by returning the samples to their centrifuge tubes and increasing the centrifuge speed (50, 100, 200, 400, 800 $\times g$). Sample composition was calculated based on the moisture loss and the initial composition. By assuming a linear gradient in both φ and Π_{ext}, Π_{ext} was calculated as:

$$\Pi_{ext} = \frac{1}{2}\overline{\rho} g_{actual} H \tag{4}$$

$\overline{\rho}$ is the mean density of the sample, g_{actual} is the actual relative centrifugal force at the sample location, and H is the height of the sample. The amount of polymer in the sample is assumed to remain constant during centrifugation. The height of the sample is thus a direct consequence of the moisture loss and can be calculated as:

$$\varphi_{init} H_{init} = \overline{\varphi} H \tag{5}$$

φ_{init} is the initial polymer volume fraction, H_{init} is the initial sample height, and $\overline{\varphi}$ is the mean polymer volume fraction after centrifugation.

2.2.8. Statistics

Error bars indicate the 95% standard error of the observation, with n indicating the number of observations.

3. Model description

3.1. Flory-Rehner theory

Swelling of cross-linked polymer gels can be described with Flory-Rehner theory. Gel swelling is characterized by the swelling pressure, Π_{swell}. At swelling equilibrium, Π_{swell} is equal to the externally applied pressure Π_{ext}. In the case of free swelling in pure water, we define $\Pi_{ext} = \Pi_{swell}$ equal to zero. There are two independent contributions to Π_{swell}: the mixing pressure Π_{mix}, and the elastic pressure Π_{elas}:

$$\Pi_{ext} = \Pi_{swell} = \Pi_{mix} - \Pi_{elas} \tag{6}$$

As has been shown for several types of food gels including soy protein gels, Π_{mix} can be described with Flory-Huggins theory (Cornet et al., 2020; Paudel, Boom, & van der Sman, 2015; Ubbink, Giardiello, & Limbach, 2007; van der Sman, 2015a). The Cloizeaux scaling law describes a more compact way of determining Π_{mix} in the semi-dilute regime (Des Cloizeaux, 1975), and has been shown successful at describing Π_{mix} for several bio-polymers (Mizrahi, Ramon, Silberberg-Bouhnik, Eichler, & Cohen, 1997; van der Sman, 2015a). The external pressures applied in our confined compression experiments are lower than those commonly used in centrifugation experiments (Cornet et al., 2020; Kocher & Foegeding, 1993; Paudel et al., 2015). Sample compositions were therefore expected to remain in the semi-dilute regime. Hence it is deemed more appropriate to use the Cloizeaux scaling law to describe Π_{mix}:

$$\frac{\Pi_{mix}\nu_w}{RT} \propto \varphi^{\beta} \tag{7}$$

ν_w is the molar volume of water, R is the universal gas constant, and T the absolute temperature. The exponent β has a value of 9/4 for dilute polymer solutions (Des Cloizeaux, 1975).

The elastic pressure, Π_{elas}, is the pressure generated upon deforming the network. We define the network deformation using the stretch parameter λ_i, where i represents the principal directions. In the freely swollen state it holds that:

$$\lambda_x = \lambda_y = \lambda_z = \lambda_0 \tag{8}$$

with λ_0 as λ_i in the freely swollen sate. In uni-axial compression with lateral confinement, λ_x and λ_y are constant and remain equal to λ_0. λ_z does vary and can be expressed in terms of λ_0, the sample height H, and the height in the freely swollen state H_0:

$$\lambda_z = \lambda_0 \frac{H}{H_0} \tag{9}$$

Network deformation is directly related to the polymer volume fraction, φ, and the polymer volume fraction in the reference state, φ_{ref}:

$$\lambda_0 \lambda_0 \lambda_z = \frac{\varphi_{ref}}{\varphi} \tag{10}$$

λ_0 relates directly to the composition of the fully swollen network as follows from the incompressibility condition:

$$\lambda_0 = \frac{\varphi_{ref}}{\varphi_0}^{1/3} \tag{11}$$

with φ_0 as the polymer content in the freely swollen state, and φ_{ref} as the polymer content in the reference state. The reference state refers to the composition at which the polymer chains are in the relaxed state (Quesada-Pérez, Maroto-Centeno, Forcada, & Hidalgo-Alvarez, 2011; van der Sman, 2015b). There is no generally accepted method to define or determine φ_{ref} (Quesada-Pérez et al., 2011). van der Sman (2015a) showed that for may bio-polymers φ_0 and φ_{ref} are related via:

$$\varphi_0 = 2/3 \varphi_{ref} \tag{12}$$

with φ_0 as the polymer volume fraction at maximum swelling. We have recently found an alternative relation between φ_0 and φ_{ref} for soy protein gels (Cornet et al., 2020). However, when fitting φ_{ref} to φ as function of Π_{ext}, the value $\varphi = \varphi_0$ ($\Pi_{ext} \approx 0$) was excluded. Since in the confined compression experiments, φ remains relatively close to φ_0, it was deemed more appropriate to use Eq. (12) to determine φ_{ref}. Swelling relative to the reference state can be expressed as $\tilde{\varphi}$:

$$\tilde{\varphi} = \frac{\varphi}{\varphi_{ref}} \tag{13}$$

A schematic representation of the stretches and their relation to $\tilde{\varphi}$ is

presented in Fig. 3.

The mechanical stress resulting from network deformation is determined using the Neo-Hookean model for the strain energy function:

$$W = \frac{1}{2} G_{ref} \left[\lambda_x^2 + \lambda_y^2 + \lambda_z^2 - 3 \right] \tag{14}$$

with W as the internal mechanical energy and G_{ref} as the shear modulus in the reference state. G_{ref} is related to φ_{ref} via (Horkay & Zrínyi, 1982):

$$G_{ref} \propto \phi_{ref}^{\beta} \tag{15}$$

The stress along the axial direction is given by (van der Sman, 2015b):

$$\begin{aligned} \sigma_{zz} &= \tilde{\varphi} \lambda_z \frac{\delta W}{\delta \lambda_z} \\ &= G_{ref} \tilde{\varphi} \lambda_z^2 \\ &= \Pi_{elas} \end{aligned} \tag{16}$$

3.2. Determination of fluxes

Local mechanical equilibrium is assumed, meaning the gradient in pressures within a volume element is zero:

$$\nabla \Pi = 0 \tag{17}$$

with Π as the sum of all pressures. The application of an external pressure Π_{ext} greater than the swelling pressure Π_{swell} will result in a pressure gradient $\nabla \Pi$ between the swollen gel and the exterior. The flux is then given by Darcy's law:

$$-j = D_s \frac{\nabla \Pi}{\nu_w RT} \tag{18}$$

where j is the flux and D_s is the self-diffusion coefficient of water. The diffusion coefficient in Eq. (18) is proportional to the ratio between the permeability and viscosity (Bisschops, Ch, Luyben, & Van Der Wielen, 1998). D_s is a function of φ (Tokita & Tanaka, 1991):

$$D_s = D_{s,0} \alpha \varphi^{-\sqrt{\beta}} \tag{19}$$

with $D_{s,\,0}$ as the self-diffusion coefficient of pure water α is a constant with value 0.013 and was estimated based on Drozdov and deClaville Christiansen (2017). β is a constant with value 9/4. Note that this will diverge when φ approaches zero. It is inserted into the continuity equation:

$$\partial_t \phi = -\partial_z j \tag{20}$$

The following assumptions and boundary conditions complete the model:

- No friction occurs between the piston, cylinder, and gel
- The piston and all side walls are impermeable
- The plate upon which the gel rests is perfectly permeable (zero resistance)
- The chemical potential of water in the bath, μ_{bath}, equals 0

The model was solved in the Lagrangian framework, moving with the polymer network. A rectangular geometry was used with the same dimensions and initial composition as used experimentally, and consisted of 10 volume elements. Spatial derivatives were computed using Finite Differences. Time integration was done using the Euler forward method.

3.2.1. Simulation approaches

Two main simulation approaches were used. The first simulation approach used the experimentally measured external pressure as a model input in which case the simulation was run continuously (from $t = 0$ until $t = t_{end}$). As described in Section 2.2.5, an overshoot in the applied load occurred during the step-change in the experiments. This led to the use of a second simulation approach in which the step-change was not simulated. Instead, the average composition determined experimentally from the piston height directly after the step change was introduced to the model after each step-change. As will be discussed in Section 4.1 there were differences in composition between volume elements. To ensure these differences were maintained after the experimental composition was introduced, we assumed the same gradient in φ as before the step change, but with the new averaged value of φ as determined from the new experimental piston height. The gradient in φ after the step-change was calculated for each volume element i as:

$$\varphi_i = \frac{V_{p,i}}{V_{p,i} + f_{w,i} \cdot \left(\left(V_p / \overline{\varphi} \right) - V_p \right)} \tag{21}$$

with $f_{w,i}$ as the fraction of the total water in the gel before the step change, V_p as the total volume of protein in the gel, and $V_{p,i}$ as the volume of protein in volume element i. $\overline{\varphi}$ is the experimental polymer volume fraction after the step-change.

4. Results and discussion

A confined compression cell was used to apply a sequence of increasing external pressures to swollen soy protein isolate (SPI) gels and model meat analogues. The external pressures applied are shown on

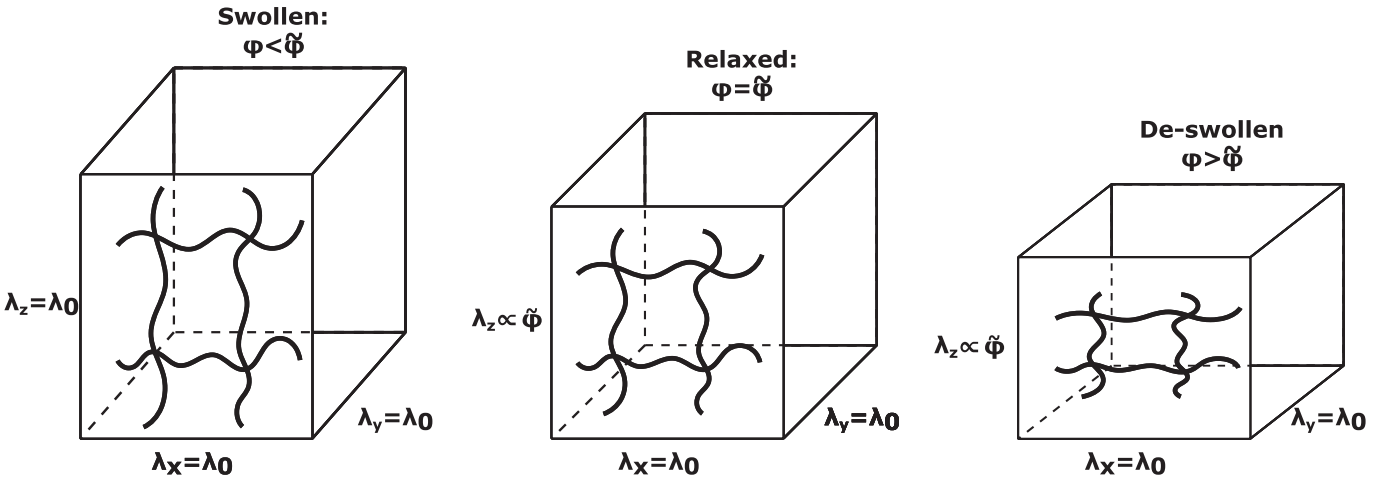

Fig. 3. After free swelling, all three stretch parameters are equal to λ_0. During uni-axial confined compression, λ_x and λ_y remain equal to λ_0, while λ_z changes proportionally with $\tilde{\varphi}$ (Eq. (9)).

the right axis of Fig. S1. The fluxes determined for the SPI gels will be discussed first, followed by the change in composition during compression. The flux and composition of the model meat analogues come next. Water mobility distributions were determined before and after swelling, and after applying an external pressure through centrifugation and will be discussed. The results are followed by a general discussion.

4.1. Confined compression of soy protein gels

The step-wise increase in external pressure during the confined compression of swollen SPI gels resulted in a repeating flux profile, as calculated using Eq. (2) (Fig. 4). The effect of dry matter content (DMC) before gelation on the flux was limited as indicated by the similarity in fluxes for gels with different DMCs. The different gels also showed qualitatively similar behaviour and will, therefore, be discussed together (Fig. 4). The flux was high shortly after an increase in external pressure and quickly decayed. The high initial flux is partly due to the overshoot in applied pressure, as discussed in Section 2.2.5. The non-zero fluxes at the end of each step in external pressure indicate that the 5 min periods of constant external pressure were too short to achieve swelling equilibrium. Direct comparison with earlier studies on the equilibrium WHC would thus not provide meaningful insight. The expulsion of water led to an increase in polymer volume fraction, φ (Fig. S1). The experimental composition increased in a manner that could be expected based on the determined fluxes. The change in composition was fast shortly after the applied pressure increased, and slowed down afterwards. This fast and slow compositional change was seen for each consecutive step in external pressure for all three tested protein concentrations.

The flux was simulated using a model based on Flory-Rehner theory and the work by Tokita and Tanaka (1991) (Section 3). The experimentally measured external pressures were used as an input for the simulation, which enables direct comparison of the simulated and experimental results (Fig. 4; black circles). The simulated fluxes are in good agreement with the experimentally measured fluxes when the external pressure is constant. However, the model did underestimate the flux directly after an increase in external pressure despite using the experimentally measured external pressures as a model input. Due to the consecutive step-changes, the underestimations accumulated. This led to an increasing underestimation of the polymer volume fraction, as shown in Fig. S1. By omitting the step change, as explained in Section 3.2.1, reasonable agreement between the experimental and simulated composition was achieved (Fig. 5). This confirms that the discrepancy between simulated and experimental fluxes during the short period after a change in load is the origin of the difference in the composition in Fig. S1.

There is generally good agreement between the experimental and simulated results when the external pressure is constant. This suggests that the model can provide a reasonable estimate of the flux for systems like soy protein gels. Furthermore, it indicates that the permeability based on the work by Tokita and Tanaka (1991) provides a reasonable estimate of the permeability. We do note that there was only a limited effect of DMC on the flux as seen both experimentally and in the simulations. This suggests that the relative importance of the change in permeability due to the change in polymer content is limited in this regime (Eq. (19)).

The compositional change in the individual volume elements during simulated confined compression can be insightful (Fig. 6). During the 5 min periods of constant external pressure, the moisture was primarily expelled from the area near the surface, as indicated by the relatively large changes in φ near the surface (high z) compared to the elements further from the surface (low z). As time progressed, moisture from areas further from the surface of the gel had travelled through, and out of the gel, and led to more widespread compositional changes. Omitting the step-change in the simulations (as explained in Section 3.2.1) had only a minor effect on the local composition (Fig. 6b) compared to when the

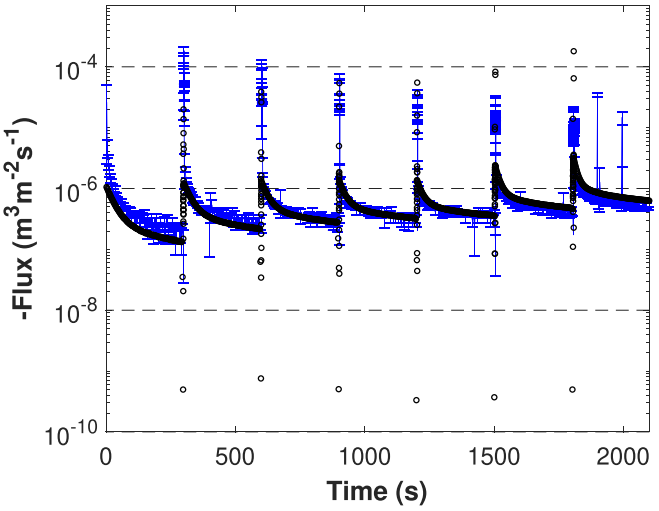

(a) 25 wt%

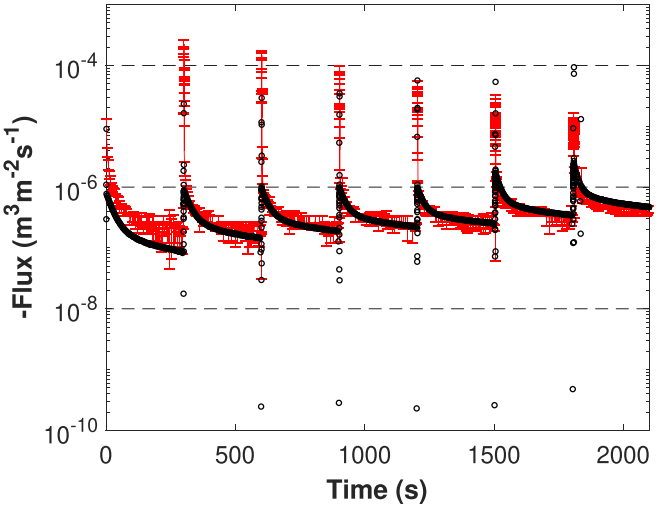

(b) 30 wt%

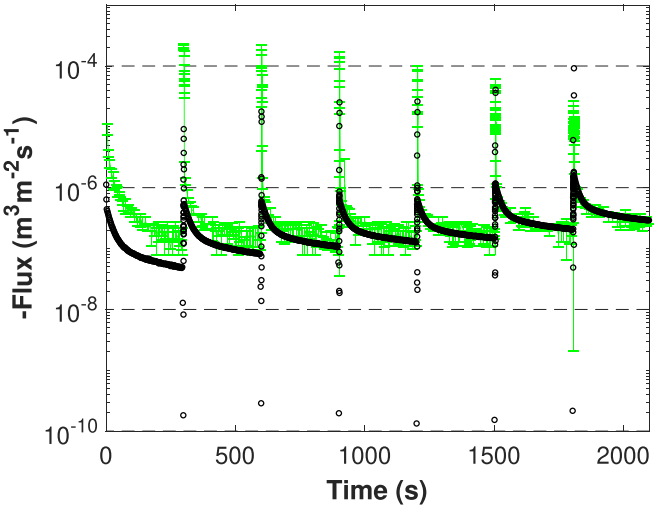

(c) 35 wt%

Fig. 4. Water release rates as determined with confined compression of swollen soy protein isolate gels. Compositions are presented with Fig. 5. Black circles are model simulations assuming identical geometry and initial composition, and using the experimentally measured external pressure as model input. $n = 3$ for the experimental fluxes.

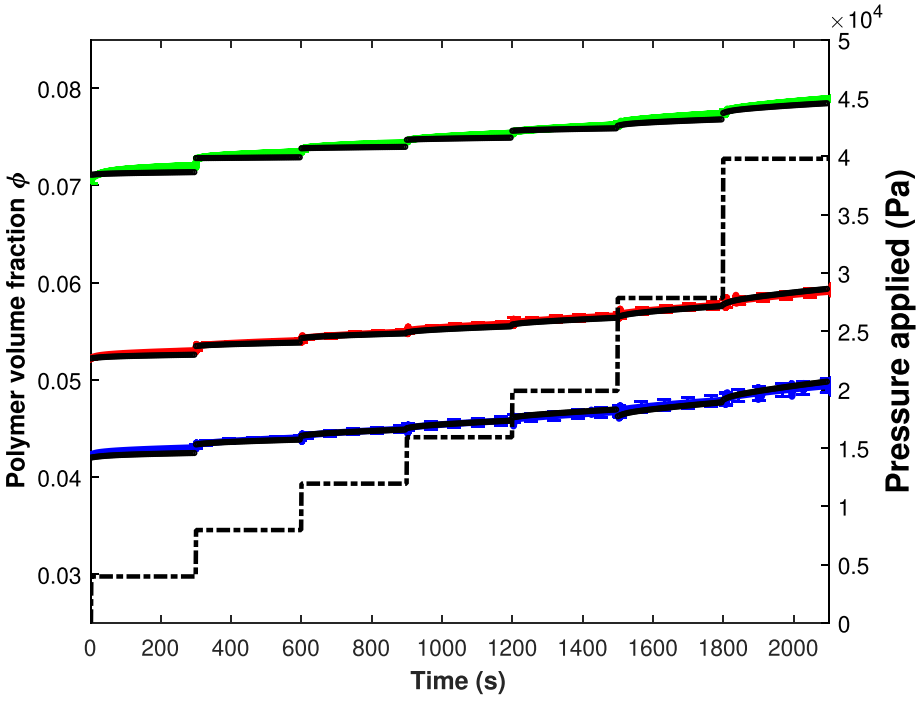

Fig. 5. Polymer volume fractions (φ) of swollen soy protein gels during confined compression experiments (n = 3). Initial levels of swelling (φ_0) were 0.042±0, 0.052±0 and 0.072±0 with initial DMCs of 25.1±0.0 wt%, 30.3±0.0 wt% 35.4±0.1 wt% (n = 3). Solid black lines are model simulations. The experimental φ shortly after a load increase was used as a model input to bypass the period of high flux (Section 3.2.1). Simulated fluxes are presented in Fig. S3. The dash-dotted line is the applied load.

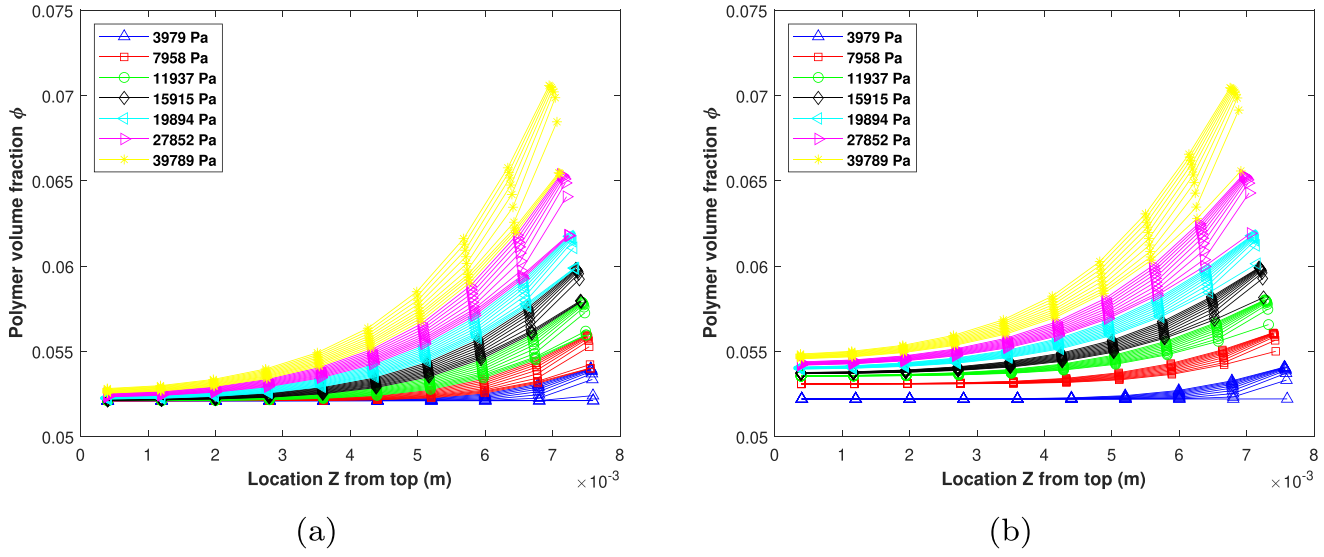

Fig. 6. Composition during simulated confined compression from the continuous approach including the step-changes (6a), and the discontinuous approach omitting the step-change in external pressure (6b). Composition is presented at the center of each volume element relative to the top of the sample ($Z(top) = 0$) for a 30 wt% SPI gel. Data is presented at 30 s intervals.

simulations were run continuously (Fig. 6a). As the local differences in φ were limited, the effect on the local pressure gradients and permeability is considered to be minor. This is in line with the reasonable agreement found for both flux (Fig. S3) and composition (Fig. 5).

4.2. Confined compression of a model meat analogue

A swollen model meat analogue was compressed using the confined compression cell. The model meat analogue swelled less than a neat soy protein gel with comparable initial DMC. This can be explained by the lower swelling capacity of gluten and mechanical interaction between soy and gluten through which gluten limits soy's ability to swell (Cornet et al., 2020). We present a single representative data set for improved clarity; duplicates can be found in Supplementary Figs. S2 and S4.

The experimentally measured flux for a model meat analogue follows a similar profile as the soy protein gels with fast and slow regimes (Fig. 7). However, the initial fast regime appears to be longer compared to the soy protein gels. Furthermore, the flux is more irregular during the first three compression steps ($\Pi_{ext} \approx$ 4, 8 and 12 kPa). Inspection of the raw force and deformation data suggests that the irregular flux is due to the fast release of water from the samples (Fig. S5). The fast water release resulted in fast dissipation of the external pressure, making it difficult for the texture analyser to maintain a constant external pressure. Stick-slip is an unlikely cause for the noise as the sample was never stationary and responded as soon as the load increased (Fig. S5).

The measured fluxes were generally higher than those found for the

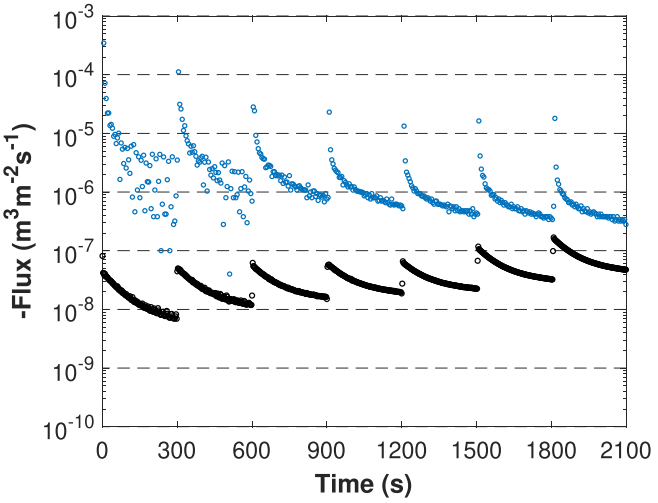

Fig. 7. Experimental flux from a swollen model meat analogue with an initial DMC of 31 wt% (blue circles). Black circles are the simulated flux of a homogeneous gels with identical dimensions using the experimental force as a model input. (For interpretation of the references to color in this figure legend, the reader is referred to the web version of this article.)

swollen SPI gels (Fig. 4). This is interesting given the much higher polymer content of the swollen model meat analogues compared to the swollen gels ($\varphi_0 = 0.17$ versus 0.04–0.08) (Fig. 5). The higher polymer content of the swollen meat analogue would have led to a decreased permeability based on Eq. (19). A lower flux compared to the gels was, therefore, expected. Moreover, the flux decreased as the external pressure increased, while the opposite would be expected based on Eq. (18) due to the greater pressure gradient. Polymer content did increase during compression (Fig. S2), which would have decreased the permeability by up to approximately 40% (Eq. (19)). However, this limited reduction in permeability cannot fully explain the reduction in flux when the applied pressure was increased.

Since the change in composition is effectively an integral of the fluxes, the qualitative change of the model meat analogue resembles that of the soy protein gels, with periods of fast change followed by a longer period of slower change (Fig. S2). The first three steps in external pressure have longer periods of fast change compared to the subsequent steps and the soy protein gels.

The simulations underestimated the experimentally determined fluxes by up to two orders of magnitude (Fig. 7). As a result of the low simulated fluxes, also the compositional change was gravely underestimated (Fig. S2). The simulated fluxes increased as the applied load was increased, while the experimental results show an opposite trend. The discrepancy between the experimental and simulated fluxes thus decreases as the experiment progresses. For the simulations, an isotropic material was assumed, while meat analogues are anisotropic materials. Although they could be considered isotropic along a single axis, the anisotropy could have affected the permeability. Furthermore, the material was assumed to be homogeneous and composed of soy protein alone, while the model meat analogues used in the experiments also contained gluten. The presence of gluten was expected to lead to a lower flux due to its lower swelling capacity (Cornet et al., 2020; Grabowska et al., 2014). Given the higher polymer content and thus lower permeability of the model meat analogues compared to the SPI gels, a lower flux was expected. Since a higher flux was measured experimentally, the model meat analogue might have features that allow for water to be released faster by providing it with a path of low resistance. Structural features capable of channelling water are internal cavities, which are known to be present in meat analogues (Dekkers et al., 2018; Schreuders et al., 2019; Wang et al., 2018).

4.3. Time domain nuclear magnetic resonance (TD-NMR)

Time-domain NMR (TD-NMR) was used to study the different water populations present in the soy protein gels and model meat analogues. The relaxation time and relative size of the different water populations can provide information on a material's internal structure (Mariette, 2009). Different water populations can be identified based on their relaxation time, T_2, which is a measure for water mobility. A short T_2 corresponds to immobile water closely associated with proteins while a longer T_2 can correspond to water in the protein matrix, inside internal cavities, or free water outside the sample. Here, i is used to distinguish between water populations in a sample, starting with $i = 1$ for the shortest relaxation time until $i = n$ for the longest.

The non-swollen SPI gels have two main relaxation times, which can be attributed to two different water populations (Fig. 8a). Population $T_{2,1}$ has a relaxation time of 4–6 and probably corresponds to protons closely associated with the protein. $T_{2,2}$ has a longer relaxation time of 20–35 ms and accounts for the rest of the signal. $T_{2,2}$ shifts to shorter relaxation times with increasing polymer concentration, which suggests this population corresponds to the water inside the polymer matrix.

After gel swelling, the relative intensity of $T_{2,1}$ (approx. 6 ms) has reduced. Since the amount of protein is taken to be constant, the reduction in relative intensity can be attributed to the increased water content. The relaxation time of $T_{2,2}$ has increased to 100–200 ms due to the increased water content of the samples. A third minor population $T_{2,3}$ was observed for the swollen SPI gels with a relaxation time of 600–1000 ms. Additional experiments indicated that population $T_{2,3}$ originated from water on the surface of the glass tube as the signal persisted after removing the sample from the tube (data not shown). $T_{2,3}$ is, therefore, considered an artefact.

The non-swollen model meat analogue has two main water populations with similar relaxation times as the non-swollen SPI gel with a similar DMC (30 wt%; Fig. 8b). This could be expected based on their similar composition and comparable DMC. Upon swelling the water mobility distribution of the model meat analogue shows similar qualitative changes as the SPI gels. The shift towards longer relaxation times is, however, less extensive ($T_{2,1} \approx$ 4 ms; $T_{2,2} \approx$ 50 ms), which can be explained by the lower water uptake during swelling. In addition to the shift, also an additional population appeared in the model meat analogues. This population, $T_{2,3}$, has a markedly longer relaxation time of approximately 570 ms and is relatively intense compared to $T_{2,3}$ seen in the swollen SPI gels.

Meat analogues can contain (air-filled) cavities after production (Wang et al., 2018, Dekkers et al., 2018, Schreuders et al., 2019). These cavities can be filled with water during swelling, as was found using X-Ray Tomography (voxel size 7 μm; data not shown). Given its high mobility and moderate intensity, population $T_{2,3}$ is thought to correspond to the water present inside internal cavities. Fibrous SPI-gluten based model meat analogues contain approximately 6–7 vol% of air (Schreuders et al., 2019), which is comparable to the intensity of the signal (Fig. 9). There is an additional minor population $T_{2,4}$ visible. Whether this population corresponds to water in larger cavities or water on the surface of the sample or NMR tube was not confirmed experimentally.

The effect of external pressure on water population $T_{2,3}$ in the swollen model meat analogues was assessed by applying a centrifugal load. Any change in the fraction of total water in population $T_{2,3}$ will provide information on whether the water from population $T_{2,3}$ is expelled at a similar pressure as population $T_{2,2}$. A range of loads was applied by increasing the centrifugal speed. Fig. 9 shows that populations $T_{2,2}$ and $T_{2,3}$ are released at different pressures. Population $T_{2,3}$ first makes up approximately 5% of total water, while after applying 10 kPa, this is reduced to approximately 2%. This shows that population $T_{2,3}$, which is associated with the water in internal cavities, is released at a lower pressure than the population $T_{2,2}$. This is in agreement with Fig. 7, where the flux reduces at pressures over 10 kPa. The remaining 2

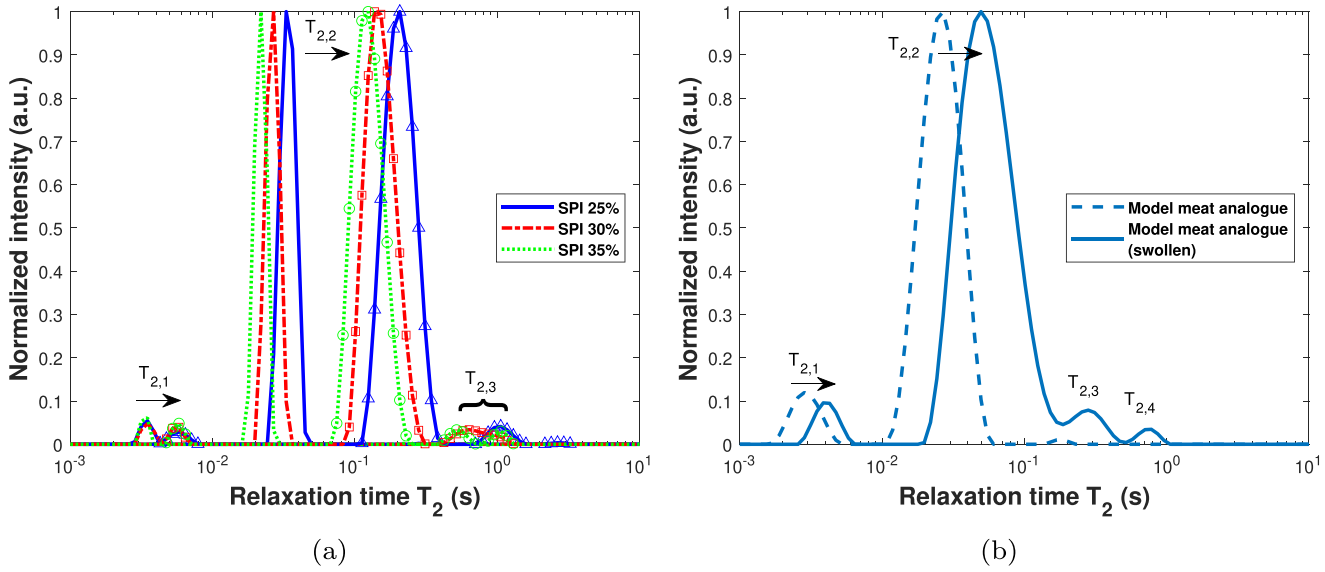

Fig. 8. CONTIN fits of the T_2 relaxation of SPI gels (8a) and model meat analogues before and after swelling (8b). The arrows indicate the shift upon swelling. Individual representative data sets were plotted data ($n = 3$).

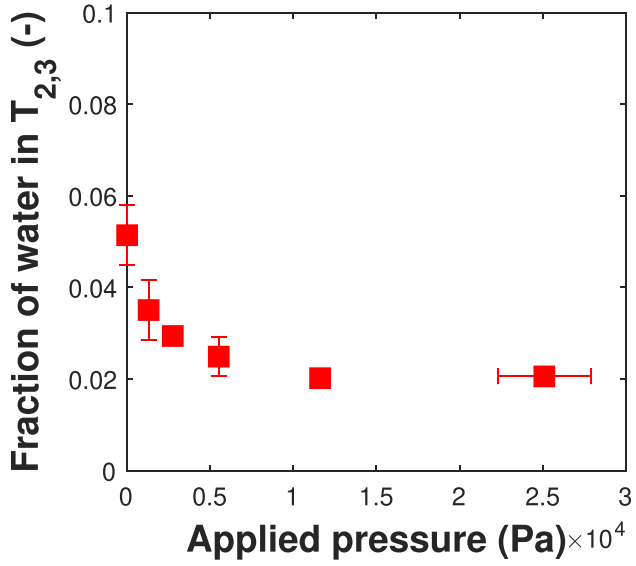

Fig. 9. Relative contribution of water population $T_{2,3}$ to the total signal as a function of applied centrifugal load for swollen model meat analogues ($n = 4$).

% of water present in population $T_{2,3}$ suggests that some of the cavities did not fully collapse. The fraction appears to be constant at 2% of total water. This suggests that the pore space is initially more easily deformed. After reaching 2%, the pore space deforms at the same rate as the rest of the matrix.

4.4. General discussion

Confined compression was used to study the water release from swollen soy protein gels and model meat analogues. A range of external pressures was applied with step-change transitions between the different pressures. The confined compression cell gave reproducible results that for homogeneous SPI gels were in reasonable to good agreement with the simulated fluxes when the external pressure was constant (Fig. 4). However, slight overshoots in external pressure did lead to a discrepancy between the experimental and simulated composition results (Fig. S1). By omitting the step-change in the simulations, however, good agreement was achieved (Fig. 5). The origin of the discrepancy was not identified. A reviewer suggested we compare the pressures applied during our confined compression with the pressures exerted by the molars during mastication. To our knowledge there are at present no studies where the mastication of meat analogues was reported. During the mastication of other foods of varying hardness De Boever, McCall, Holden, and Ash (1978) recorded an average load of approximately 13 N. When assuming a contact area of 3 cm^2, the average pressure was approximately 43 kPa, which is comparable to the maximum pressure applied during our experiments (up to 40 kPa).

Model meat analogues with a more complex structure and composition were also analysed with the confined compression cell. Although the interpretation of the results did require input from other methods such as TD-NMR, the confined compression cell did provide new insights into the water release from meat analogues. The measured fluxes were much higher than could be expected for a material with such a polymer content (Fig. 7). This suggested that the model meat analogue had features capable of channelling the water. These features were identified as internal water-filled cavities using TD-NMR (Fig. 8b), as indicated by the presence of a water population with a long relaxation time ($T_{2,3}$). The cavities could provide a low-resistance path for water and thus explain the high measured fluxes. Upon compression, the volume fraction of cavities reduced (Fig. 9), rendering a more homogeneous gel as in the case of SPI. This could explain why for higher external pressures the flux reduced to a level closer to simulated result. Some cavities may persist at higher loads, which can explain why the flux remains at a higher level than the simulations. The numerical simulations of the model meat analogue showed that they do not behave as homogeneous gels, which is expected to be due to the internal cavities. A sensory study by Aaslyng et al. (2003) on the juiciness of pork showed that the factors responsible for the perceived juiciness change during mastication. They concluded that meat juices are most important during the first few chews, while salivation by the consumer is also of importance during prolonged mastication. Confined compression of model meat analogues showed that the initial juice release is fast, but that it rapidly reduces. The simulated compositional gradients for the SPI gels showed that moisture is mainly released from the areas near the surface. This effect will be less pronounced in meat analogues due to the greater connectivity offered by the internal cavities. Furthermore, during mastication structural breakdown occurs. This will reduce the distance the juice will have travel to be released, and could further increase the juice release rate. As

the food breaks down the timescale at which water release occurs therefore also becomes smaller. This suggests that different parts of the release rate curves may be relevant as mastication progresses.

Internal cavities can provide a way for water, and meat analogue juices, to be released at a higher rate. They could, therefore, be desired in a meat analogue products as they may enhance the initial juiciness. Incorporating greater quantities of air could increase this effect. Furthermore, the shape and orientation of the cavities could influence the magnitude and persistence of the effect. Elongated and highly connected channels parallel with the axis of compression may not collapse during compression and could enhance the release rate over longer periods and at higher loads. Several recent studies showed that elongated channels are present in meat analogues and that the level of elongation depends on the shear rate and temperature during processing in a shear cell (Dekkers et al., 2018; Schreuders et al., 2019; Wang et al., 2018). An alternative approach to create such elongated channels is through directional freezing during post-processing (Fukushima, 1981). Juiciness could be enhanced through the intelligent design of the meat analogue structure, although the correlation with sensory perceived juiciness is to be confirmed. The use of confined compression as an analytical tool could help in this process.

5. Conclusions

We have investigated the use of confined compression in food science by studying the water release from soy protein gels and meat analogues. The water release kinetics from swollen soy protein gels can be measured with confined compression and simulated with good accuracy using models based on Flory-Rehner theory and the framework proposed by Tokita when the external pressure is constant. Confined compression of model meat analogues showed much higher fluxes due to the presence of inernal water-filled cavities. TD-NMR results showed that these cavities largely disappear as loads increase. Some cavities, however, persist and could explain why the experimental flux remains greater than the simulations. This study has shown that the water release from meat analogue products depends on their internal structure. By controlling the internal structure, the perception of juiciness could be enhanced. Confined compression was proven to be a promising tool to study food gels.

Industrial relevance

Meat analogues could offer a more sustainable alternative to real meat. However, some of the sensory qualities of meat analogues, such as the juiciness, can still be improved. Juiciness relates to the product's water release properties, which we studied using a confined compression cell. This method is new in food science and provides insight into the rate at which water is released from the product. Our results showed that meat analogues release water faster than would be expected based on their composition. Additional experiments with time-domain NMR indicated that the meat analogues contain water-filled cavities. These cavities can explain the faster release of water as they provide little resistance to the flow of water. The effect of internal cavities on water release suggests that changing the internal cavities in meat analogues could affect their water release properties, and potentially improve their juiciness. Confined compression might, therefore, offer a new physical method to measure juiciness, although a direct comparison with sensory juiciness should still be made. The new insight into the role of cavities in water release could help product and process developers to improve their products.

Declaration of Competing Interest

There are no conflicts to declare.

Acknowledgements

We acknowledge Remco Hamoen, Marleen Verburg, and the Technical Development Studio for their part in designing and manufacturing the compression cell. We acknowledge Frank Vergeldt for his assistance with the TD-NMR experiments. This research is part of the project Plant Meat Matters, which is co-financed by Top Consortium for Knowledge and Innovation Agri & Food by the Dutch Ministry of Economic Affairs; the project is registered under contract number TKI-AF-16011.

Appendix A. Supplementary data

Supplementary data to this article can be found online at https://doi.org/10.1016/j.ifset.2020.102528.

References

Drozdov, A. D., & deClaville Christiansen, J. (2017). A simplified model for equilibrium and transient swelling of thermo-responsive gels. *Journal of the Mechanical Behavior of Biomedical Materials, 75*, 20–32. https://doi.org/10.1016/J.JMBBM.2017.06.034

Hoek, A. C. (2010). Will Novel Protein Foods beat meat? Consumer acceptance of meat substitutes - a multidisciplinary research approach. PhD thesis, Wageningen UR. URL http://library.wur.nl/WebQuery/clc/1926634.

Pearson, A. M., & Dutson. (1994). *Quality attributes and their measurement in meat, poultry and fish* (1 ed.). Dordrecht: Springer Science+Business Media.

Aaslyng, M. D., Bejerholm, C., Ertbjerg, P., Bertram, H. C., & Andersen, H. J. (2003). Cooking loss and juiciness of pork in relation to raw meat quality and cooking procedure. *Food Quality and Preference, 14*(4), 277–288. https://doi.org/10.1016/S0950-3293(02)00086-1. URL. ISSN 09503293 https://www.sciencedirect.com/science/article/pii/S0950329302000861.

Aiking, H. (2011). Future protein supply. *Trends in Food Science and Technology, 22*(2), 112–120. https://doi.org/10.1016/j.tifs.2010.04.005

Bertram, H. C., Aaslyng, M. D., & Andersen, H. J. (2005). Elucidation of the relationship between cooking temperature, water distribution and sensory attributes of pork - a combined NMR and sensory study. *Meat Science, 70*(1), 75–81. https://doi.org/10.1016/j.meatsci.2004.12.002. ISSN 03091740.

Bertram, H. C., Andersen, H. J., & Karlsson, A. H. (2001). Comparative study of low-field NMR relaxation measurements and two traditional methods in the determination of water holding capacity of pork. *Meat Science, 57*(2), 125–132. https://doi.org/10.1016/S0309-1740(00)00080-2. ISSN 0309-1740.

Bertram, H. C., Dønstrup, S., Karlsson, A. H., & Andersen, H. J. (2002). Continuous distribution analysis of T2 relaxation in meat—An approach in the determination of water-holding capacity. *Meat Science, 60*, 279–285. https://doi.org/10.1016/S0309-1740(01)00134-6. ISSN 03091740.

Bisschops, M. A. T., Ch, K., Luyben, A. M., & Van Der Wielen, L. A. M. (1998). Generalized Maxwell-Stefan approach for swelling kinetics of dextran gels. *Industrial and Engineering Chemistry Research, 37*(8), 3312–3322. https://doi.org/10.1021/ie9800389. ISSN 08885885.

Cornet, S. H. V., Snel, S. J. E., Lesschen, J., van der Goot, A. J., & van der Sman, R. G. M. (2021). Enhancing the water holding capacity of model meat analogues through marinade composition. *Journal of Food Engineering, 290*, 110283. https://doi.org/10.1016/j.jfoodeng.2020.110283

Cornet, S. H. V., van der Goot, A. J., & van der Sman, R. G. M. (2020). Effect of mechanical interaction on the hydration of mixed soy protein and gluten gels. *Current Research in Food Science, 3*, 134–145. https://doi.org/10.1016/j.crfs.2020.03.007

De Boever, J. A., McCall, W. D., Holden, S., & Ash, M. M. (1978). Functional occlusal forces: An investigation by telemetry. *The Journal of Prosthetic Dentistry, 40*(3), 326–333. https://doi.org/10.1016/0022-3913(78)90042-2. ISSN 00223913.

Dekkers, B. L., Hamoen, R., Boom, R. M., & van der Goot, A. J. (2018). Understanding fiber formation in a concentrated soy protein isolate - pectin blend. *Journal of Food Engineering, 222*, 84–92. https://doi.org/10.1016/j.jfoodeng.2017.11.014

Dekkers, B. L., Nikiforidis, C. V., & van der Goot, A. J. (2016). Shear-induced fibrous structure formation from a pectin/SPI blend. *Innovative Food Science and Emerging Technologies, 36*, 193–200. https://doi.org/10.1016/j.ifset.2016.07.003

Des Cloizeaux, J. (1975). The Lagrangian theory of polymer solutions at intermediate concentrations. *Journal de Physique, 36*(4), 281–291.

Flory, P. J., & Rehner, J. (1943). Statistical mechanics of cross-linked polymer networks II. Swelling. *The Journal of Chemical Physics, 11*(11), 521–526. https://doi.org/10.1063/1.1723792

Fukushima, D. (1981). Soy proteins for foods centering around soy sauce and tofu. *Journal of the American Oil Chemists' Society, 58*(3), 346–354. https://doi.org/10.1007/BF02582376. ISSN 0003021X.

Grabowska, K. J., Tekidou, S., Boom, R. M., & van der Goot, A. J. (2014). Shear structuring as a new method to make anisotropic structures from soy-gluten blends. *Food Research International, 64*, 743–751. https://doi.org/10.1016/j.foodres.2014.08.010. ISSN 09639969.

Grabowska, K. J., Zhu, S., Dekkers, B. L., de Ruijter, N. C. A., Gieteling, J., & van der Goot, A. J. (2016). Shear-induced structuring as a tool to make anisotropic materials using soy protein concentrate. *Journal of Food Engineering, 188*, 77–86. https://doi.org/10.1016/j.jfoodeng.2016.05.010

Horkay, F., & Zrínyi, M. (1982). Studies on the Mechanical and Swelling Behavior of Polymer Networks Based on the Scaling Concept. 4. Extension of the Scaling Approach to Gels Swollen to Equilibrium in a Diluent of Arbitrary Activity. *Macromolecules, 15*(5), 1306–1310. https://doi.org/10.1021/ma00233a018

Knapp, D. M., Barocas, V. H., Moon, A. G., Yoo, K., Petzold, L. R., & Tranquillo, R. T. (1997). Rheology of reconstituted type I collagen gel in confined compression. *Journal of Rheology, 41*(5), 971–993. https://doi.org/10.1122/1.550817. ISSN 0148-6055.

Kocher, P. N., & Foegeding, E. A. (1993). Microcentrifuge-based method for measuring water-holding of protein gels. *Journal of Food Science, 58*(5), 1040–1046. https://doi.org/10.1111/j.1365-2621.1993.tb06107.x. ISSN 17503841.

Krintiras, G. A., Diaz, J. G., van Der Goot, A. J., Stankiewicz, A. I., & Stefanidis, G. D. (2016). On the use of the Couette cell technology for large scale production of textured soy-based meat replacers. *Journal of Food Engineering, 169*, 205–213. https://doi.org/10.1016/j.jfoodeng.2015.08.021

Liu, Q., Subhash, G., & Moore, D. F. (2011). Loading velocity dependent permeability in agarose gel under compression. *Journal of the Mechanical Behavior of Biomedical Materials, 4*(7), 974–982. https://doi.org/10.1016/j.jmbbm.2011.02.009

Lucherk, L. W., O'Quinn, T. G., Legako, J. F., Rathmann, R. J., Brooks, J. C., & Miller, M. F. (2017). Assessment of objective measures of beef steak juiciness and their relationships to sensory panel juiciness ratings. *Journal of Animal Science, 95*(6), 2421–2437. https://doi.org/10.2527/jas2016.0930. ISSN 15253163.

Mariette, F. (2009). Investigations of food colloids by NMR and MRI. *Current Opinion in Colloid and Interface Science, 14*(3), 203–211. https://doi.org/10.1016/j.cocis.2008.10.006

Mizrahi, S., Ramon, O., Silberberg-Bouhnik, M., Eichler, S., & Cohen, Y. (1997). Scaling approach to water sorption isotherms of hydrogels and foods. *International Journal of Food Science and Technology, 32*(2), 95–105. https://doi.org/10.1046/j.1365-2621.1997.00379.x. ISSN 09505423.

Paudel, E., Boom, R. M., & van der Sman, R. G. M. (2015). Change in water-holding capacity in mushroom with temperature analyzed by Flory-Rehner theory. *Food and Bioprocess Technology, 8*(5), 960–970. https://doi.org/10.1007/s11947-014-1459-7. ISSN 19355149.

Provencher, S. W. (1984). Contin: A general purpose constrainded regularization program for inverting noisy linear algebraic and integral equations. *Computer Physics Communications, 35*, 818–819. https://doi.org/10.1016/s0010-4655(84)82935-5. ISSN 00104655.

Quesada-Pérez, M., Maroto-Centeno, J. A., Forcada, J., & Hidalgo-Alvarez, R. (2011). Gel swelling theories: the classical formalism and recent approaches. *Soft Matter, 7*(22), 10536. https://doi.org/10.1039/c1sm06031g. ISSN 1744-683X.

Roos, R. W., Petterson, R., & Huyghe, J. M. (2013). Confined compression and torsion experiments on a pHEMA gel in various bath concentrations. *Biomechanics and Modeling in Mechanobiology, 12*(3), 617–626. https://doi.org/10.1007/s10237-012-0429-0. ISSN 16177959.

Schreuders, F. K. G., Bodnár, I., Erni, P., Boom, R. M., & van der Goot, A. J. (2020). Water redistribution determined by time domain NMR explains rheological properties of dense fibrous protein blends at high temperature. *Food Hydrocolloids, 101*. https://doi.org/10.1016/j.foodhyd.2019.105562. ISSN 0268005X.

Schreuders, F. K. G., Dekkers, B. L., Bodnár, I., Erni, P., Boom, R. M., & van der Goot, A. J. (2019). Comparing structuring potential of pea and soy protein with gluten for meat analogue preparation. *Journal of Food Engineering, 261*(May), 32–39. https://doi.org/10.1016/j.jfoodeng.2019.04.022. ISSN 02608774.

van der Sman, R. G. M. (2007). Moisture transport during cooking of meat: An analysis based on Flory-Rehner theory. *Meat Science, 76*(4), 730–738. https://doi.org/10.1016/j.meatsci.2007.02.014. ISSN 03091740.

van der Sman, R. G. M. (2015a). Biopolymer gel swelling analysed with scaling laws and Flory-Rehner theory. *Food Hydrocolloids, 48*, 94–101. https://doi.org/10.1016/j.foodhyd.2015.01.025

van der Sman, R. G. M. (2015b). Hyperelastic models for hydration of cellular tissue. *Soft Matter, 11*, 7579–7591. ISSN 1744-683X.

Smetana, S., Mathys, A., Knoch, A., & Heinz, V. (2015). Meat alternatives life cycle assessment of Most known meat substitutes. *The International Journal of Life Cycle Assessment, 1254–1267*. https://doi.org/10.1007/s11367-015-0931-6, 2050. ISSN 0948-3349.

Soltz, M. A., & Ateshian, G. A. (1998). Experimental verification and theoretical prediction of cartilage interstitial fluid pressurization at an impermeable contact interface in confined compression. *Journal of Biomechanics, 31*(10), 927–934. https://doi.org/10.1016/S0021-9290(98)00105-5. ISSN 00219290.

Tian, B., Wang, Z., van der Goot, A. J., & Bouwman, W. G. (2018). Air bubbles in fibrous caseinate gels investigated by neutron refraction, X-ray tomography and refractive microscope. *Food Hydrocolloids, 83*, 287–295. https://doi.org/10.1016/j.foodhyd.2018.05.006

Tokita, M., & Tanaka, T. (1991). Friction coefficient of polymer networks of gels. *The Journal of Chemical Physics, 95*(6), 4613–4619. https://doi.org/10.1063/1.461729. ISSN 00219606.

Ubbink, J., Giardiello, M. I., & Limbach, H. J. (2007). Sorption of water by bidisperse mixtures of carbohydrates in glassy and rubbery states. *Biomacromolecules, 8*(9), 2862–2873. https://doi.org/10.1021/bm0701898. ISSN 15257797.

Van Oeckel, M. J., Warnants, N., & Boucqué, C. V. (1999). Comparison of different methods for measuring water holding capacity and juiciness of pork versus on-line screening methods. *Meat Science, 51*(4), 313–320. https://doi.org/10.1016/S0309-1740(98)00123-5. ISSN 03091740.

Wang, Z., Tian, B., van der Goot, A. J., & Boom, R. (2018). Air bubbles in calcium caseinate fibrous material enhances anisotropy. *Food Hydrocolloids, 87*, 497–505. https://doi.org/10.1016/j.foodhyd.2018.08.037

Warner, R. D. (2017). The Eating Quality of Meat-IV Water Holding Capacity and Juiciness. In *Lawrie's Meat Science* (8th ed., pp. 419–459). Woodhead Publishing.

Winger, R. J., & Hagyard, C. J. (1994). Juiciness - its importance and some contributing factors. In A. M. Pearson, & T. R. Dutson (Eds.), *Quality attributes and their measurement in meat, poultry and fish products* (1st ed., pp. 94–124). Dordrecht: Springer Science+Business Media.